Soil Power? Can Microbial Fuel Cells Power Non-Trivial Sensors?

Gabriel Marcano
UC San Diego
Computer Science and Engineering
gmarcano@ucsd.edu

Pat Pannuto
UC San Diego
Computer Science and Engineering
ppannuto@ucsd.edu

ABSTRACT

This paper explores the power delivery potential of soil-based microbial fuel cells. We build a prototype energy harvesting setup for a soil microbial fuel cell, measure the amount of power that we can harvest, and use that energy to drive an e-ink display as a representative example of a periodic energy-intensive load. Microbial fuel cells are highly sensitive to environmental conditions, especially soil moisture. In near-optimal, super moist conditions our cell provides approximately 100 µW of power at around 500 mV, which is ample power over time to power our system several times a day. We further explore how cell performance diminishes and recovers with varying moisture levels as well as how cell performance is affected by the load from the energy harvester itself. In sum, we find that the confluence of ever lower-power electronics and new understanding of microbial fuel cell design means that "soil-powered sensors" are now feasible. There remains, however, significant future work to make these systems reliable and maximally performant.

CCS CONCEPTS

• **Hardware** → *Renewable energy*; *Platform power issues*; *Emerging architectures.*

KEYWORDS

microbial fuel cell (MFC), biobattery, energy harvesting, low power

ACM Reference Format:
Gabriel Marcano and Pat Pannuto. 2022. Soil Power? Can Microbial Fuel Cells Power Non-Trivial Sensors?. In *1st ACM Workshop on No Power and Low Power Internet-of-Things (LP-IoT'21), January 31-February 4, 2022, New Orleans, LA, USA.* ACM, New York, NY, USA, 6 pages. https://doi.org/10.1145/3477085.3478989

1 INTRODUCTION

Power is a perennial challenge for real-world sensor deployments. To support scale, devices need to last long periods of time with little to no supporting infrastructure or maintenance. Existing wide-area sensing systems rely on batteries or harvest the required energy, most often from solar or wind sources. One problem with solar, wind, and other common sources of power is that they are not always available or reliable. This has led to growing interest in new, non-traditional energy scavenging sources.

The burgeoning set of low-power energy harvesting chips now available can harvest power from voltage sources as low as 25 mV.[1] While most of these energy harvesters target thermoelectric, piezoelectric, RF, and solar energy sources, their ability to extract power from low-voltage sources facilitates the exploration of novel energy sources, like tree trunks [6], and the re-visitation of old ideas, such as microbial fuel cells (MFCs). MFC harvesting has been studied in wastewater management [1, 11, 24], but there has not been a similar focus for soil MFCs. We re-examine the viability of soil MFCs to produce sufficient power to be useful for sensor applications. Specifically, due to the low but relatively constant power available, we find that soil MFCs may be a good fit for the new "reliable but intermittent" sensor class [6].

MFCs are made of electrogenic bacteria that release electrons as they metabolize their food. Normally, these bacteria use metals in the soil as electron acceptors, but it is possible to get them to grow on an electrically conductive anode, which allows us to capture the electrons they expel. As the source of power is the activity of living organisms, MFC performance can vary drastically based on local environmental conditions, which we will explore empirically in Section 5. Towards real-world applications, then, this paper is just step one. We explore a best-case MFC to see if it is capable of powering modern sensors. We see a long line of exciting future work towards the question of what it would take to realize viable and reliable MFCs everywhere.

Before diving in, we wish to draw distinction between MFCs as a new energy scavenging opportunity versus MFCs as a new "renewable" energy source. Logan et al. [14] argue for the standardization of terminology when describing MFCs. Specifically, unless the medium or nutrients than an MFC uses to generate electricity are refreshed somehow, the apparatus should be referred to as a *biobattery* rather than a fuel cell. In the long term, we are interested in embedding MFCs in environments such as agricultural beds or wetlands, where extant processes can restore nutrients. The cell we study in this work, however, is self-contained. Thus, it is a biobattery, and we will refer to it as such moving forward.

2 BACKGROUND

MFCs have been studied for over a century. In his 1911 work, Potter [19] presents one of the earliest experiments using microbial activity to generate and measure electric potential. The yeast and bacteria used for these early experiments were grown in a sterilized, nutrient-enriched solution placed in a glass container and porous cylinder connected to platinum electrodes. To understand MFC operation, we explore major developments in MFC design since these first experiments.

In 1963, NASA explored the possibility of using human wastewater as a source of power [1]. Early results showed that there was

[1]Examples include the MCRY12-125Q-42DI and related chips from MATRIX.

LP-IoT'21, January 31-February 4, 2022, New Orleans, LA, USA

ACM ISBN 978-1-4503-8702-6/22/01.
https://doi.org/10.1145/3477085.3478989

some energy available for extraction. The most notable contribution from this work was the advent of incubation, a now-standard process that establishes bacterial colonies in hyper-favorable conditions before deployment.

In the early 1990s Habermann and Pommer did pioneering work in long-running MFCs. They demonstrated a system that ran for five years with no maintenance (beyond feeding). Their design featured an aqueous MFC configuration that stabilized the pH level, which enabled long term function so long as the cell continued to receive external sugar wastewater as fuel [5, 24]. This design showed how to develop a system capable of processing waste products from electrogenic bacteria to support longitudinal operation.

Many previous MFC designs incorporated mediators, which are slightly toxic and expensive artificial compounds that facilitate the transfer of electrons from bacteria to the anode [20, 27]. Research in the late 1990s showed that mediators are not required to construct MFCs as some bacteria have natural mechanisms to expel electrons [9]. Removing mediators simplifies MFC construction and reduces cost, which makes this approach more common for modern cells, including ours.

For MFCs without mediators, bacteria from the genus *Geobacter* dominate the anode of soil MFCs, and their presence is correlated with higher power production [21, 28]. One design consequence of this taxon is that the anode must be in an anaerobic environment, as *Geobacteriaceae* are almost completely obligate anaerobes [13]. These bacteria are common in many soils and subsurface environments [15], so much so that no special effort is required to acquire them for use in soil MFCs. Early work identified that waterlogging soil works to exclude oxygen from the buried anode [4]. We use this same waterlogging approach to promote an anaerobic environment around the anode buried under the soil in our biobattery.

Many materials can be used for the cathode and anode of MFCs. Examples range from mercury and platinum [4, 19], to graphite felt [17], to tungsten carbide on reduced graphene oxide nanolayers [18], and many more [24]. When selecting materials, Josephson highlights that galvanic corrosion can confound electrical measurements [8], as galvanic corrosion is also a potential source of power [6]. To build a renewable soil MFC (rather than an earth battery [2]), then, care must be taken to select materials for the electrodes that are galvanically inert.

Looking forward, one of the biggest open questions we will face when trying to deploy soil MFC-powered sensors is an absence of extant, longitudinal studies. There are a few experiments and deployments that span months to years [5, 25]. However, we are unable to find any commercial deployments of MFCs as power source. One hypothesis suggests that inefficiencies introduced by current MFC construction make their use in industry infeasible [24]. Still, more recent studies describe sensor applications which use MFCs for power, and demonstrate that it is now possible to architect low-power sensor nodes powered off solely a biobattery [16, 22]. In this work, we focus on the biobattery and harvesting operation itself, to understand how we might look to both maximize and stabilize power for future long-term deployments.

3 PROTOTYPE DESIGN

Figure 1 provides an overview of the architecture and realization of our prototype system. For our biobattery we use a commercial off-the-shelf Mudwatt that uses galvanically inert carbon felt electrodes [8]. Soil composition is known to have significant affect on soil MFC performance [3, 26], so we use commercial soil with known parameters for our cell (Figure 1c for details).

To grow the initial colony, we follow the instructions provided by the Mudwatt. We place 1 cm of soil in the container and then install the anode at that level. We then bury the anode below an additional 5 cm of soil. Finally, we place the cathode on top of the soil, where it is exposed to the ambient air. The Mudwatt required approximately three weeks of constant watering to mature and produce consistent power.

After reaching maturity, with a constant 2.2 kΩ load our Mudwatt produces 100 µW of power in steady-state. The peak open-circuit voltage we observe is around 700 mV. This limits the energy harvesters we can use. Following the 2021 survey done by Jagtap [6], we choose an ADP5091 development kit to harvest power from the Mudwatt. We configure the ADP5091 to have its main boost enabled, the regulated out voltage set to 2.5 V, the LDO mode enabled, the boost mode on, the regulated output enabled, and the MPPT sensing function enabled and in the dynamic mode.

We use a 330 mF supercapacitor as our energy store. We choose a supercapacitor for its nearly unbounded cycle count as well as being able to tolerate non-constant voltages when charging. We estimate that this supercapacitor should provide the system with 390 mJ of energy when discharging from 2.6 V to 2.1 V. From the expected power draw of system components, shown in Table 1, we estimate a single event will require about 160 mJ, which leaves ample overhead.

We select the Redboard Artemis for our microcontroller as it features an Ambiq Apollo3 MCU. In principle, the Apollo3 draws just 6 µW when in deep sleep. It also integrates an ultra-low-power RTC, which allows for efficiently scheduling wake-ups far in the future [7]. To reduce unnecessary power draw, we remove the indicator LEDs and the UART bridge from the Redboard.

We use an e-ink display screen refresh as a representative example of a periodic high-energy task sensors might undertake. Examples of other periodic tasks include wireless transmission or on-device machine learning[12]. E-ink displays draw little to no power when holding an image, but they consume an appreciable amount of energy to refresh their display. For instance, our display, per its datasheet, draws a maximum of 40 mW over four seconds to refresh its display. As the e-ink display controller is not optimized for deep sleep performance, we add a power switch to explicitly disconnect power to the e-ink display when not in use.

4 IMPLEMENTATION

Figure 1b shows our actual prototype. The Mudwatt is connected to the `VIN` and ground terminals on the ADP5091 development kit, and the supercapacitor is connected to the battery terminals of the harvester. Once the supercapacitor is charged, we manually disconnect the ADP5091 harvester from the supercapacitor and connect the supercapacitor to the `Vcc` and ground rails of the breadboard. This powers the Redboard and the e-ink display. More importantly,

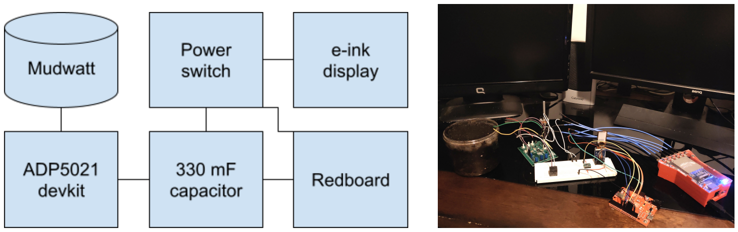

(a) Prototype block diagram. **(b) Prototype system.**

Biobattery	Magical Microbes Mudwatt [17]
6 cm soil	Miracle-Gro: Cactus, Palm, & Citrus Potting Mix 0.06% total nitrogen, 0.02% P_2O_5, 0.04% K_2O
Harvester	ADP5091-1-EVALZ
Supercapacitor	FMC0H334ZF (330 mF)
Microcontroller	SparkFun RedBoard Artemis
Power switch	TPS22860DBVR
E-ink interface	DESPI-C102
E-ink display	GDEW0102I3F, 1.02 inch display
Precision logger	RocketLogger [23]

(c) Components used to build prototype system.

Figure 1: Prototype Overview & Implementation. In (b), from left to right: the Mudwatt, the AD5091 harvester development kit, the supercapacitor, the e-ink display and power switch, the Redboard Artemis, and the RocketLogger.

this "unloads" the biobattery during operation. As we will see in Section 5, unloading the cell for windows of time has serious impact on the cell behavior. A future design might include a dedicated switch to support this behavior, but properly handling cold-start for such a design is challenging and outside the scope of our prototype implementation's capability, hence the manual operation of this step.

Originally, we did not intend to include a dedicated power switch to gate power to the e-ink display. However, initial testing showed that the display was not shutting down as expected, thus necessitating the removal of its power supply externally. We also disable all of the pins on the Redboard to prevent the e-ink display from drawing power through the data lines.

We have uploaded the firmware for our prototype to Gitlab.[2] The firmware manages the e-ink display and the power state of the e-ink and the microcontroller. During a power-on event, the firmware first performs a full-screen refresh by enabling power to the display, sending framebuffer data to update the display with the state of the internal RTC, and finally initiating the actual refresh. The limited communication interface to the e-ink display requires polling the busy line to detect when refresh completes. This results in higher-than-anticipated power draw for the MCU during operation. A full event takes approximately four seconds to complete.

After the screen redraw, we turn power off to the e-ink display and instruct the Redboard to enter its deep sleep mode. An internal timer fires 20 seconds later to wake up the Redboard and repeat the program. The board repeats this operation until the energy reserves are depleted.

We generally attempt to keep the biobattery in optimal conditions. When not running the experiments testing the impacts of the Mudwatt drying out, we add water to the Mudwatt on an almost daily basis to ensure the anode remains in an anaerobic condition. We also let the Mudwatt rest for an hour every other day to ensure the biobattery remains in peak operating condition.

5 EARLY-STAGE RESULTS, TRENDS, AND OBSERVATIONS

Our experiments serve two primary thrusts. First, we characterize the basic performance of our biobattery. Second, we are interested to see how energy harvesting impacts the energy recovery potential of the system. As a final step, we characterize the energy demand of our implementation.

5.1 Mudwatt Characterization

To begin, we test the performance of the biobattery with a simple, fixed 2.2 kΩ load. This load selection follows guidance from impedance sweeps of prior designs [8], plus our own experimentation. In steady-state, a constantly-wet cell produces a little over 100 µW continuously.

Next, in Figure 2a we consider what one might expect to be 'normal' environmental conditions for a deployed biobattery. Cells will dry out over time, but precipitation or irrigation events will occur reasonably often. This healthy, untaxed cell exhibits both a logarithmic decay as it dries under load and logarithmic recovery when water is introduced. Qualitatively, the decay and recovery of the cell look similar across a modest number of trials, which invites future work that explores the predictability of energy over time.

One natural next question, what happens if water never comes? Figure 2b allows a cell to dry completely. Somewhat surprisingly, in the extreme, the cell actually reverses direction and exhibits moderate "negative" current flow. While this phenomenon is interesting, it is also three orders of magnitude lower power than our healthy, fully-functioning biobattery. Future systems may consider exploiting this for "emergency reserve" power, but it is unlikely to be sufficient for a primary energy source in the short term.

After an extreme dry-out event, the biobattery takes significantly longer to recover. As seen in Figure 2c, it takes the cell nearly four days to fully recover as opposed to roughly five hours in the modestly-dry case. Notably, this recovery curve is largely linear rather than logarithmic. Future work is needed to understand the underlying biology, but, again, qualitative empirical trials find this behavior to be consistent.

5.2 Curiosities & Observations

When water is added, we see short-term near-instantaneous spikes in output power in addition to the longitudinal response. We can see this in Figure 2c, where there are small peaks and drops at the 10, 40, 50, 60, 70, and 90 hours points which correspond to watering events. This phenomenon, if detectable via microcontroller ADC monitoring or some other circuitry, might make it possible to detect when water is added. This could, in turn, be used to predict and leverage impending periods of higher energy availability. There are

[2] https://gitlab.com/gemarcano/mudwatt/-/tree/lp-iot

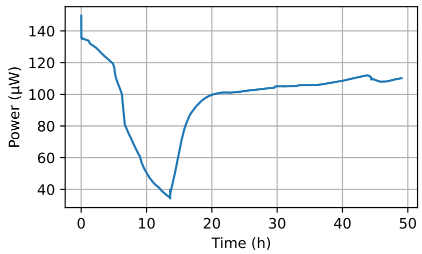

(a) Steady-state watering. We let an unloaded (open circuit) Mudwatt dry out over several days. At time 0, we connect the Mudwatt to a 2.2 kΩ resistor as a load. At around 14 h, we water the cell. The cell recovers its power output over the course of the next five hours. The graph is zoomed in to show detail; note that the y-axis does not begin at 0.

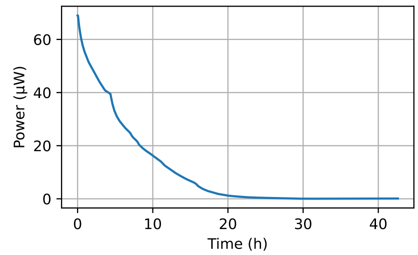

(b) Complete dry-out. Time 0 is approximately one minute after the end of Figure 2a. The load from Figure 2a remains connected. Power decreases as the cell dried out, reaching 0 µW after a day. During the final several hours, the cell polarity reverses slightly (reaching around -15 mV with -7 µA before we add water for (c)).

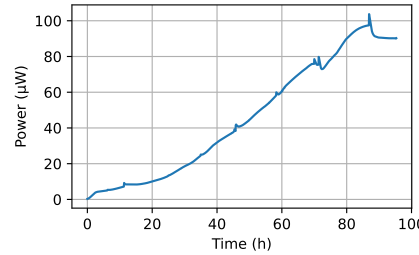

(c) Recovery from dry-out. This immediately follows the dry-out from (b). The 2.2 kΩ load resistor remains connected. At time 0, we water the cell. The small peaks and valleys in the power output are due to additional water being added to ensure the Mudwatt anode remains well submerged.

Figure 2: Power over time and sensitivity to water. With semi-regular watering, (a) shows the regular logarithmic declination and recovery of cell power during "normal" drying out. (b) and (c) show the behavior when a loaded cell is allowed to dry out completely, and the corresponding, slower, linear recovery of the cell.

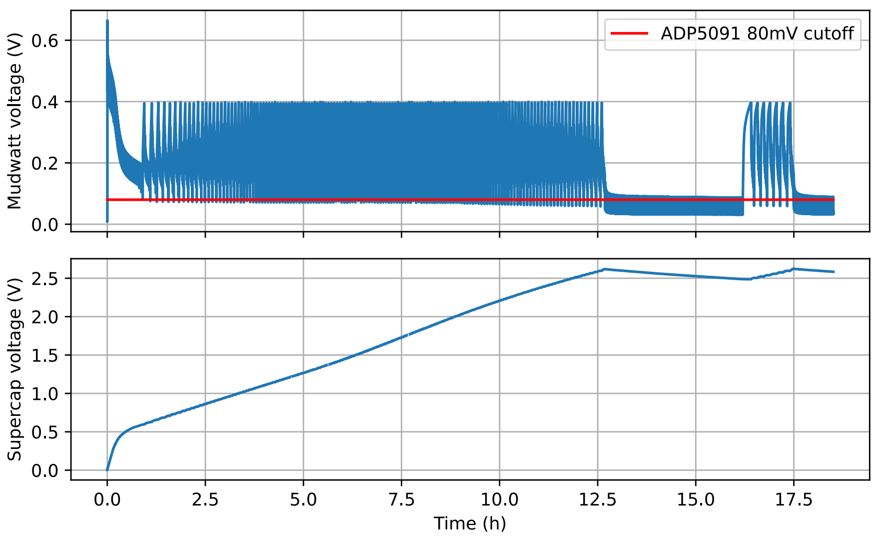

(a) Charging profile from cold-start to steady-state. The Mudwatt is fully watered and rested before beginning. The Redboard is disconnected. The supercapacitor charges to its target in just over 12.5 hours. At first, charging is quite fast, as there is built-up energy in the rested cell. During initial charging, the ADP5091 operates in "asynchronous mode,"[3]. When the input voltage dips below 80 mV, the harvester can no longer operate. The harvester restarts once input voltage exceeds the 380 mV cold-start voltage. This "input-falls-below-operation, bacteria recovers" cycle accounts for the spiky operation, shown in detail in (b). Once the target charging threshold (2.5 V plus some hysteresis margin) is reached, the harvester switches to "synchronous mode,"[3]. Here, the harvester no longer browns out, which results in a constant load on the biological cell (which never recovers) and a slow, constant drain on the storage supercapacitor. Finally, around hour 16, the energy reserve depletes enough that the harvester returns to "asynchronous mode," which causes the system as a whole to enter a macro-level steady state.

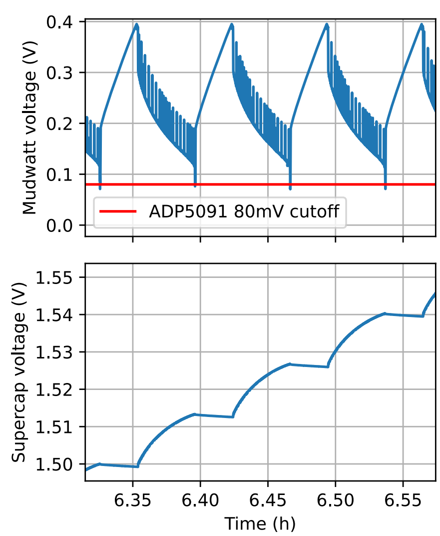

(b) Detail view of harvester cycles. At 380 mV, the cold-boot circuitry of the harvester activates, and the system begins charging. This energy demand causes the voltage on the biobattery to slowly fall. Every 16 s, the MPPT algorithm detaches the harvester for 256 ms to measure the open-circuit voltage, which accounts for the Mudwatt voltage spikes during harvesting. When input falls below 80 mV (red line in graph), the harvester shuts off. With no load, the Mudwatt begins to recover, until it reaches 380 mV and the cycle restarts. In steady state, this oscillates with a period of approximately seven minutes.

Figure 3: Mudwatt energy harvesting behavior over time. (a) shows the Mudwatt voltage as the supercapacitor is charged. (b) shows a zoomed-in portion of (a), which shows the ADP5091 shutting down and restarting as available power from the biobattery falters and recovers, along with the voltage of the supercapacitor rising as power is harvested.

possible confounds, however. Simply bumping the Mudwatt also causes small perturbations in output, and when the power output is low enough, so can airflow.

Waste buildup is a possible explanation for sensitivity to motion. The bacteria in the Mudwatt produce gas as they metabolize. We have observed that the heavier the load on the Mudwatt, the more gas bubbles form over time. Shaking or squeezing the container does result in a small spike in energy production if it violent enough to release some of the trapped gas, but it is not clear if this is because of the removal of the gas, because water is now able to enter where the gas was trapped, because the shaking helps nutrients dissolved in the water to move around, or for another reason.

In our experimentation, we also noticed that when allowed to rest (i.e. no load), the Mudwatt is able to increase its voltage above what it can sustain with an attached load. In practice, this voltage increase may translate to some additional harvestable power. In Figure 2a, the Mudwatt had been allowed to rest before the data collection began. We can see that the initial voltage was higher than the voltage the Mudwatt settled on after recovery. Furthermore, it remained at an elevated voltage for almost 10 hours after being plugged into the 2.2 kΩ load. This suggests that applications with higher instantaneous power demands may be able to buffer energy in the cell itself rather than requiring dedicated electronics.

5.3 Harvester ICs, MPPT, and MFCs

Next, we implement and evaluate the full system described previously. We attach an ADP5091 harvester to the cell and observe the ability to recover energy. As a first-order result, it takes the harvester just over 12.5 hours to charge the supercapacitor energy store to its target voltage of 2.6 V.

Figure 3 looks at charging performance in detail. The initial logarithmic charging burst in the first half hour stems from the Mudwatt being in a rested and "overcharged" state. In steady-state, charging is largely linear. The effective empirical charging rate is approximately 80 mJ/h or 20 µW. Of note, this is less than the 100 µW steady-state power draw achieved by the simple 2.2 kΩ load.

Figure 3b is a close-up of the behavior of the ADP5091. The harvester runs a maximum power point tracking (MPPT) algorithm which targets 80% of open-circuit voltage. For reference, in Figure 2a, the initial open-circuit voltage was 570 mV while the steady-stage voltage with the load is 465 mV ($\frac{465}{570} \approx 82\%$). In practice, however, this set point is too aggressive, and the cell repeatedly drains to the point of harvester failure.

To try to ameliorate the strain on the biobattery, we increase the MPPT set point. At a MPPT target of 90%, the cell takes longer to discharge below the 80 mV threshold, but it still consistently drains to the point of failure. At 95%, most of the asynchronous phase[3] of the harvester operates well. The harvester draws an average of 60 µW off the biobattery. However, as the harvester approaches the threshold to switch to its synchronous mode[3], it begins to draw significantly more power off of the cell, which again drains to the 80 mV failure point. We are unable to find any MPPT threshold that enables continuous operation of the harvester, despite the cell's ability to support a static 2.2 kΩ load at over 100 µW.

[3]The ADP5091 asynchronous and synchronous modes relate to how the harvester is powering its boost converter. In asynchronous mode, the battery is disconnected from the boost converter, which allows the battery to charge without the draw of powering the boost converter. In synchronous mode, the harvester connects the battery to the boost converter, which allows the converter to draw power from the battery to sustain its operation. See the ADP5091 datasheet for more information.

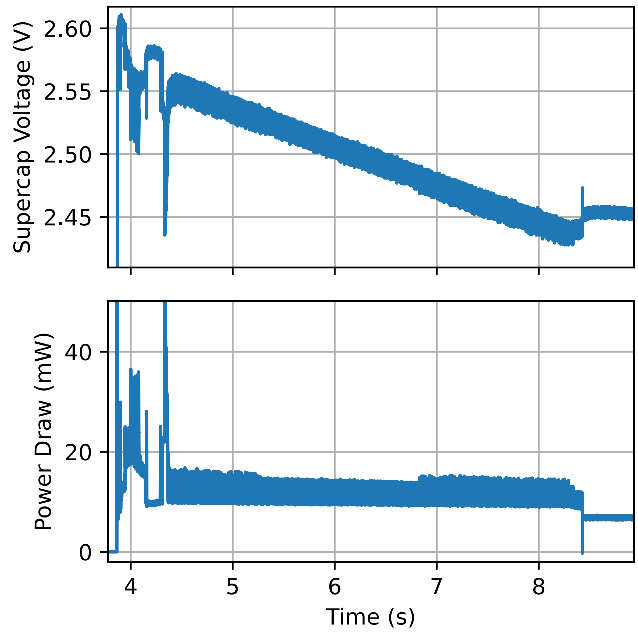

Figure 4: Supercapacitor voltage and system power draw during a screen refresh event.

Table 1: Expected and actual power draw. Not all components are active all of the time. We are not able to measure the actual power draw of the ADP5091 development kit, as it is difficult to separate the power draw due to charging the supercapacitor and the energy usage of the harvester itself.

Component	Expected (mW)	Actual (mW)
Artemis (active)	1.5	10
Artemis (sleep)	0.004	7
ADP	0.0018	-
E-ink (update)	40	4

5.4 Energy Consumption

Once the supercapacitor charges to around 2.6 V, we switch the supercapacitor from charging to providing power to the e-ink display and the MCU circuit. Figure 4 shows the overall system power, and Table 1 breaks down the measured power draw of the components.

We find several non-trivial differences between datasheet values and empirical power use. We expected significantly lower power draw from the microcontroller and more power draw from the e-ink display. We suspect that we did not successfully power down all of the auxiliary/peripheral components for the Artemis. While realizing optimal low-power states is known to be challenging [10], it is still disappointing to see how far off the largely out-of-box experience is for a development board of the current state-of-the-art lowest-power MCU.

The e-ink display demand draw consists mostly of many small spikes in power draw, which average to a lower power utilization than expected. Nonetheless, the overall energy use is still appreciable and requires continuous operation for approximately five seconds. Integrating power draw measurements, the energy consumption for a refresh of the e-ink display is 24 mJ, and the energy usage of the microcontroller for the same time period is 31 mJ. Combined, both the e-ink display and the microcontroller consume 55 mJ per e-ink display refresh.

6 FUTURE WORK

We keep our biobattery saturated with water, which yields consistent power output. Maintaining soil at saturation is unrealistic for many real-world settings, from potted plants to agricultural fields. We intend to explore MFCs with exposure to less moisture and plan to compensate for the expected decrease in power by connecting multiple MFCs in series and/or parallel. For more immediate deployment, we also hope to consider applications in wetlands, which are already near-optimal for MFC performance.

There is significant opportunity in harvester design. To start, we need to develop designs that better approximate the simple static load, which outperforms today's MPPT algorithms. In the future, it may be possible to further exploit the non-linear growth and decay of MFC power output to extract even more energy.

We know there are a myriad of environmental variables that impact the energy production of soil based MFCs, but we do not know their respective magnitudes. We plan to collect data on soil humidity, temperature, and exposure to light, to begin to identify their impact on the power output of our Mudwatt.

In this work, we study a biobattery. In contrast to MFCs, biobatteries have no way to replenish nutrients. As such, eventually the bacterial colony around the anode will deplete its nutrient supply and die out. Characterizing how long biobatteries can last can help enable plans for real-world deployment and long term use. It also helps identify what might be done to increase their longevity and could be a key step towards perpetual, renewable cells.

REFERENCES

[1] J. H. Canfield, Goldner B. H., and R. Lutwack. 1963. *Research on Applied Bioelectrochemistry, Report Nr. 1, Contract NASw-623, First Quartery Progress Report, March 14 to June 30, 1963.* Technical Report. Magna Corporation, Washington, D.C., USA.

[2] George Dieckmann. 1885. Electric earth battery.

[3] Sara J. Dunaj, Joseph J. Vallino, Mark E. Hines, Marcus Gay, Christine Kobyljanec, and Juliette N. Rooney-Varga. 2012. Relationships between Soil Organic Matter, Nutrients, Bacterial Community Structure, And the Performance of Microbial Fuel Cells. *Environmental Science & Technology* 46, 3 (2012), 1914–1922. https://doi.org/10.1021/es2032532 PMID: 22243479.

[4] Louis J Gillespie. 1920. Reduction potentials of bacterial cultures and of water-logged soils. *Soil Sci* 9, 4 (1920), 199–216.

[5] W Habermann and EH Pommer. 1991. Biological fuel cells with sulphide storage capacity. *Applied microbiology and biotechnology* 35, 1 (1991), 128–133.

[6] Dhananjay Jagtap and Pat Pannuto. 2020. Reliable Energy Sources as a Foundation for Reliable Intermittent Systems. In *Proceedings of the 8th International Workshop on Energy Harvesting and Energy-Neutral Sensing Systems* (Virtual Event, Japan) *(ENSsys '20)*. 22–28. https://doi.org/10.1145/3417308.3430276

[7] Dhananjay Jagtap and Pat Pannuto. 2021. Repurposing cathodic protection systems as reliable, in-situ, ambient batteries for sensor networks. In *Proceedings of the 20th ACM/IEEE International Conference on Information Processing in Sensor Networks, IPSN*, Vol. 21.

[8] Colleen Josephson, Neal Jackson, and Pat Pannuto. 2020. Farming Electrons: Galvanic Versus Microbial Energy in Soil Batteries. *IEEE Sensors Letters* 4, 12 (2020), 1–4. https://doi.org/10.1109/LSENS.2020.3043666

[9] Hyung Joo Kim, Sik Hyun Moon, and Hong Kim Byung. 1999. A microbial fuel cell type lactate biosensor using a metal-reducing bacterium, Shewanella putrefaciens. *Journal of Microbiology and Biotechnology* 9, 3 (1999), 365–367.

[10] Hyung-Sin Kim, Michael P. Andersen, Kaifei Chen, Sam Kumar, William J. Zhao, Kevin Ma, and David E. Culler. 2018. System Architecture Directions for Post-SoC/32-Bit Networked Sensors. In *Proceedings of the 16th ACM Conference on Embedded Networked Sensor Systems* (Shenzhen, China) *(SenSys '18)*. Association for Computing Machinery, 264–277. https://doi.org/10.1145/3274783.3274839

[11] Baikun Li, Karl Scheible, and Michael Curtis. 2011. *Electricity Generation from Anaerobic Wastewater Treatment in Microbial Fuel Cells.* Technical Report. The Water Environment Research Foundation.

[12] Ji Lin, Wei-Ming Chen, Yujun Lin, John Cohn, Chuang Gan, and Song Han. 2020. MCUNet: Tiny Deep Learning on IoT Devices. *CoRR* abs/2007.10319 (2020). arXiv:2007.10319 https://arxiv.org/abs/2007.10319

[13] WC Lin, Maddalena V Coppi, and DR Lovley. 2004. Geobacter sulfurreducens can grow with oxygen as a terminal electron acceptor. *Applied and environmental microbiology* 70, 4 (2004), 2525.

[14] Bruce E. Logan, Bert Hamelers, René Rozendal, Uwe Schröder, Jürg Keller, Stefano Freguia, Peter Aelterman, Willy Verstraete, and Korneel Rabaey. 2006. Microbial Fuel Cells: Methodology and Technology. *Environmental Science & Technology* 40, 17 (2006), 5181–5192. https://doi.org/10.1021/es0605016 PMID: 16999087.

[15] Derek R. Lovley, Toshiyuki Ueki, Tian Zhang, Nikhil S. Malvankar, Pravin M. Shrestha, Kelly A. Flanagan, Muktak Aklujkar, Jessica E. Butler, Ludovic Giloteaux, Amelia-Elena Rotaru, Dawn E. Holmes, Ashley E. Franks, Roberto Orellana, Carla Risso, and Kelly P. Nevin. 2011. Geobacter: The Microbe Electric's Physiology, Ecology, and Practical Applications. In *Advances in Microbial Physiology*, Robert K. Poole (Ed.). Advances in Microbial Physiology, Vol. 59. Academic Press, 1–100. https://doi.org/10.1016/B978-0-12-387661-4.00004-5

[16] Philipp Mayer, Michele Magno, and Luca Benini. 2018. Combining microbial fuel cell and ultra-low power event-driven audio detector for zero-power sensing in underwater monitoring. In *2018 IEEE Sensors Applications Symposium (SAS)*. 1–6. https://doi.org/10.1109/SAS.2018.8336772

[17] Magical Microbes. 2021. MudWatt: Grow a Living Fuel Cell. https://www.magicalmicrobes.com/products/mudwatt-clean-energy-from-mud Accessed June 2021.

[18] Hend Omar Mohamed, Sawsan Abo Talas, Enas T. Sayed, Sung-Gwan Park, Tasnim Eisa, Mohammad Ali Abdelkareem, Olfat A. Fadali, Kyu-Jung Chae, and Pedro Castaño. 2021. Enhancing power generation in microbial fuel cell using tungsten carbide on reduced graphene oxide as an efficient anode catalyst material. *Energy* (2021), 120702. https://doi.org/10.1016/j.energy.2021.120702

[19] M. C. Potter. 1911. Electrical Effects Accompanying the Decomposition of Organic Compounds. *Proceedings of the Royal Society of London. Series B, Containing Papers of a Biological Character* 84, 571 (1911), 260–276. http://www.jstor.org/stable/80609

[20] Sibel D. Roller, H. Peter Bennetto, Gerard M. Delaney, Jeremy R. Mason, John L. Stirling, and Christopher F. Thurston. 1984. Electron-transfer coupling in microbial fuel cells: 1. comparison of redox-mediator reduction rates and respiratory rates of bacteria. *Journal of Chemical Technology and Biotechnology. Biotechnology* 34, 1 (1984), 3–12. https://doi.org/10.1002/jctb.280340103 arXiv:https://onlinelibrary.wiley.com/doi/pdf/10.1002/jctb.280340103

[21] Miriam A Rosenbaum and Ashley E Franks. 2014. Microbial catalysis in bioelectrochemical technologies: status quo, challenges and perspectives. *Applied microbiology and biotechnology* 98, 2 (2014), 509–518.

[22] Maurizio Rossi, Pietro Tosato, Luca Gemma, Luca Torquati, Cristian Catania, Sergio Camalò, and Davide Brunelli. 2017. Long range wireless sensing powered by plant-microbial fuel cell. In *Design, Automation Test in Europe Conference Exhibition (DATE), 2017*. 1651–1654. https://doi.org/10.23919/DATE.2017.7927258

[23] Lukas Sigrist, Andres Gomez, Roman Lim, Stefan Lippuner, Matthias Leubin, and Lothar Thiele. 2016. RocketLogger - Mobile Power Logger for Prototyping IoT Devices. In *14th ACM Conference on Embedded Networked Sensor Systems.*

[24] Anthony J. Slate, Kathryn A. Whitehead, Dale A.C. Brownson, and Craig E. Banks. 2019. Microbial fuel cells: An overview of current technology. *Renewable and Sustainable Energy Reviews* 101 (2019), 60–81. https://doi.org/10.1016/j.rser.2018.09.044

[25] Tonia Tommasi and Giorgia Lombardelli. 2017. Energy sustainability of Microbial Fuel Cell (MFC): A case study. *Journal of Power Sources* 356 (2017), 438–447. https://doi.org/10.1016/j.jpowsour.2017.03.122

[26] Ning Wang, Zheng Chen, Hong-Bo Li, Jian-Qiang Su, Feng Zhao, and Yong-Guan Zhu. 2015. Bacterial community composition at anodes of microbial fuel cells for paddy soils: the effects of soil properties. *Journal of Soils and Sediments* 15, 4 (2015), 926–936.

[27] Lemuel B. Wingard, Ching Hao Shaw, and James F. Castner. 1982. Bioelectrochemical fuel cells. *Enzyme and Microbial Technology* 4, 3 (1982), 137–142. https://doi.org/10.1016/0141-0229(82)90104-1

[28] Matthew D Yates, Patrick D Kiely, Douglas F Call, Hamid Rismani-Yazdi, Kyle Bibby, Jordan Peccia, John M Regan, and Bruce E Logan. 2012. Convergent development of anodic bacterial communities in microbial fuel cells. *The ISME journal* 6, 11 (2012), 2002–2013.